Polymer 50 (2009) 2775–2785

Contents lists available at ScienceDirect

Polymer

journal homepage: www.elsevier.com/locate/polymer

Biodegradable comb-dendritic tri-block copolymers consisting of poly(ethylene glycol) and poly(L-lactide): Synthesis, characterizations, and regulation of surface morphology and cell responses

Feirong Gong [a], Xiaoyan Cheng [a], Shanfeng Wang [b,*], Yang Wang [c], Yun Gao [a], Shujun Cheng [a,**]

[a] Key Laboratory for Ultrafine Materials of Ministry of Education, School of Materials Science and Engineering, East China University of Science and Technology, Shanghai 200237, China
[b] Department of Materials Science and Engineering, The University of Tennessee, Knoxville, TN 37996, USA
[c] Shanghai Medical College, Fudan University, 138 Yi-xue-yuan Road, Shanghai 200032, China

ARTICLE INFO

Article history:
Received 22 February 2009
Received in revised form
12 April 2009
Accepted 21 April 2009
Available online 3 May 2009

Keywords:
Polylactide
Comb-dendritic tri-block copolymer
Cell responses

ABSTRACT

A series of well-defined dumbbell-shaped tri-block copolymers consisting of comb-like poly(L-lactide) (PLLA) and linear poly(ethylene glycol) (PEG) with narrow molecular weight distributions and varied PLLA arm lengths have been synthesized via the sequential preparation of terminal dendronized polyhydric PEG and ring-opening polymerization (ROP) of L-lactide (LA). The terminal dendronized polyhydric PEG was prepared by the conjugation of amine-terminated fourth-generation polyester dendrons with NHS-activated PEG followed by the deprotection of acetonide groups. The length of PLLA arms can be readily controlled by the feed molar ratio of LA monomer to the hydroxyl groups in PEG macroinitiator. Differential scanning calorimetric (DSC) measurements and thermal gravimetric analysis (TGA) have been performed to indicate that the glass transition temperature (T_g), melting point (T_m), degree of crystallinity (χ_c), and onset decomposition temperature (T_d) of the copolymers are lower than those of the linear polylactide (LPLLA). Self-organized porous structures have been found in the copolymer films after solution casting and solvent evaporation. Honeycomb-like surface morphology could be achieved by adjusting the length of PLLA arms. Meanwhile, surface chemistry of the copolymer films such as surface hydrophobicity and the capability of adsorbing protein increase with the length of PLLA arms. Controllable material properties have been correlated with the *in vitro* cell responses. No cytotoxicity of the dumbbell-shaped copolymers has been found using rabbit bone marrow stromal cells (BMSCs). Human embryonic kidney (HEK) 293T cells have been used to reveal the effect of surface characteristics on cell attachment and proliferation. It has been found that cell proliferation has been enhanced significantly on the surfaces of the copolymers with longer PLLA arm lengths because of more favorable surface physicochemical properties.

1. Introduction

Aliphatic polyesters such as poly(L-lactide) (PLLA), polyglycolide (PGA), poly(ε-caprolactone) (PCL) and their copolymers have been widely used for pharmaceutical and tissue-engineering applications because of their biodegradability, low immunogenicity, and good biocompatibility [1–7]. Among these biomedical applications, drug delivery is one important aspect as numerous drugs, growth factors, and antibodies need to be locally delivered to induce tissue regeneration [8–12]. PLLA and its copolymers suffer from some disadvantages such as strong hydrophobicity, poor cell affinity [13], high crystallinity, and difficulty in controlling polymer degradation [14]. In addition, local acidity increases during the degradation of PLLA and makes the release profiles of drugs and biomacromolecules deviate from the sustained release behavior, which is usually called as "polyphasic" or "biphasic" [15,16]. To overcome the above-mentioned problems, some approaches such as introducing hydrophilic units to the PLLA backbone and designing branched structures have been used [17–23]. Many branched macromolecular architectures such as comb [24], star [25,26], and graft polymers [27–29] containing PLLA have been synthesized.

Poly(ethylene glycol) (PEG) is a widely used hydrophilic polymer with low cytotoxicity, hemolyticity, and non-immunogenicity [30]. Introduction of PEG blocks to hydrophobic PCL or PLLA not

* Corresponding author. Tel.: +1 865 974 7809; fax: +1 865 974 4115.
** Corresponding author. Tel.: +86 21 6425 2050; fax: +86 21 6425 2855.
E-mail addresses: swang16@utk.edu (S. Wang), chshj2003@yahoo.cn (S. Cheng).

0032-3861/$ – see front matter © 2009 Elsevier Ltd. All rights reserved.
doi:10.1016/j.polymer.2009.04.033

only improves polymer hydrophilicity but also modifies mechanical and biochemical properties. Thus PEG-based amphiphilic block copolymers and linear di-block, tri-block, and multi-block copolymers of PLLA and PEG have been extensively investigated [31–34].

Linear PLLA (LPLLA) can be rationally synthesized by the means of ring-opening polymerization (ROP) of L-lactide (LA) initiated by Stannous(II) 2-ethylhexanoate ($Sn(Oct)_2$). Despite the ROP mechanism and the initiating complex remain elusive, they are considered to be alcohol-initiated [35–38] because the degree of polymerization is dependent on the monomer-to-alcohol ratio [39] and the produced polymers are hydroxyl terminated. Based on this mechanism, star-like and dendritic PLLA can be synthesized with multi-functional initiators [40–43]. These copolymers with many shorter PLLA arms have unique properties such as lower molecular weight distribution [44], better hydrophilicity and faster biodegradation compared with LPLLA having the same molecular weight. Meanwhile, the branched structure of these copolymers may offer a solution to improve the "polyphasic" or "biphasic" release profiles in LPLLA [17–23].

Dumbbell-shaped or comb-dendritic block copolymers have been achieved using a variety of methods [45–50]. In this paper, we present the synthetic route and detailed characterizations of novel amphiphilic dumbbell-shaped tri-block copolymers with comb-shaped PLLA end arms and linear PEG center block connected using aliphatic polyester dendrons. These dendronized linear polymers provide an alternative dendritic architecture with a variety of aspect ratios accessible depending on the length of the PLLA arms and PEG block, and the generation of the polyester dendrons. Using this architecture, we have achieved high-molecular-weight copolymers with narrow molecular weight distribution as well as improved hydrophilicity with a high multiplicity of functional groups. In order to explore their tissue-engineering applications, these unique comb-dendritic tri-block copolymers have been investigated and compared with LPLLA on regulating cell responses through their controllable surface characteristics.

2. Experimental

2.1. Materials

L-lactide (LA, PURAC Biochem, Netherlands) was recrystallized twice from anhydrous ethyl acetate and dried under vacuum at room temperature. $Sn(Oct)_2$ was purchased from Sigma–Aldrich Co. (Milwaukee, WI) and distilled twice under a reduced pressure prior to use. α,ω-Bis(2-carboxyethyl)-poly(ethylene glycol) (PEG diacid) with a weight-average molecular weight (M_w) of 10,000 g/mol and a polydispersity index (PDI) of 1.03 was obtained from Fluka and dehydrated by azeotropic distillation in toluene before use. Dowex 50W X2-100 H^+ resin and 2,2-bis(hydroxymethyl) propionic acid (bis-MPA) were purchased from Acros. Dicyclohexylcarbodiimide (DCC), *N*,*N*-carbonyldiimidazole (CDI), *N*-hydroxysuccinimide (NHS), and 4-dimethylaminopyridine (DMAP) were from GL Biochem Ltd. (Shanghai, China) and used as received; 4-(dimethylamino) pyridinium *p*-toluene sulfonate (DPTS) was synthesized according to the literature [51]. Amine-terminated fourth-generation polyester dendron (G4-NH_2) was synthesized according to a previous method of using a divergent route based on acetonide-protected bis-MPA [46,49]. This method was proved to be efficient for preparing aliphatic polyester dendrons because of the high reactivity of anhydrides and easy purification of the obtained product. The purity of the synthesized G4-NH_2 was examined by gel permeation chromatography (GPC). The GPC retention curve was highly symmetric and the molecular weight distribution was as narrow as 1.01. Other reagents were commercially available and used as received. All solvents were thoroughly dried and distilled before use.

2.2. Synthesis of amine-terminated fourth-generation polyester dendron (G4-NH_2)

The fourth-generation polyester dendron (G4-$CO_2CH_2C_6H_5$) was prepared from bis-MPA by a divergent route [46,49]. The amine-terminated dendron was synthesized by transferring the benzyl ester group at the root of dendron to the primary amino group through catalytic hydrogenolysis followed by the reaction of the carboxyl groups at the root of the dendron with an excess amount of 1,3-diaminopropane in the presence of a catalyst CDI. ^1H NMR ($CDCl_3$) δ: 4.32–4.24 (CH_2, 28H), 4.14–3.57 (CH_2, 32H), 3.41 (CH_2, 2H), 2.96 (CH_2, 2H), 1.82 (CH_2, 2H), 1.41–1.36 (CH_3, 48H), 1.29–1.17 (CH_3, 45H). All the data in this step were consistent with the literature [46,49].

2.3. Synthesis of NHS-activated PEG

PEG–diacid (10 g, 1 mmol) and 1.16 g of NHS (10 mmol) were dissolved in 50 mL of dichloromethane (CH_2Cl_2) in an oven-dried flask and treated with 2.08 g of DCC (10 mmol), 0.12 g of DMAP (1 mmol), and 1.1 g of DPTS (3.7 mmol) for 48 h at room temperature. After solid dicyclohexylurea (DCU) byproduct was removed by filtration, the filtrate was precipitated in 1 L of chilled ether. The obtained polymer was then re-dissolved in CH_2Cl_2 and the solution was centrifuged at −5 °C, 13,000 rpm for 1 h to remove the residue of the catalyst. After precipitated in chilled ether and dried under vacuum at room temperature for 24 h, NHS-activated PEG was obtained as white powder with a yield of over 90%.

2.4. Synthesis of fourth-generation dendronized PEG (PEG-G4 dendron)

For the coupling reaction of PEG with the polyester dendron, 3.47 g (0.34 mmol) of NHS-activated PEG and 4.37 g (2.04 mmol) of G4-NH_2 were dissolved in 25 mL CH_2Cl_2. After 1 mL (7.33 mmol) of triethylamine ($N(Et)_3$) was added, the reaction mixture was stirred at room temperature for two days, as shown in the first step in Fig. 1. The produced mixture was precipitated in an excess of ether and filtered to afford 4.29 g of white powder product with a yield of 85%.

2.5. Synthesis of terminal dendronized PEG with 32 hydroxyl functionalities (PEG-G4-$(OH)_{32}$)

First, 1.50 g of PEG-G4 dendron was dissolved in 75 mL methanol. After one teaspoon of Dowex H^+ resin was added, the reaction mixture was stirred for 12 h at room temperature, as shown in the second step in Fig. 1. Once the reaction was complete, Dowex H^+ resin was filtered off and washed with a small amount of methanol. The methanol solution was condensed to ~15 mL and precipitated in 250 mL of diethyl ether to give 1.13 g of the product as white crystals.

2.6. Synthesis of dumbbell-shaped tri-block copolymer

As shown in the third step in Fig. 1, the dumbbell-shaped tri-block copolymers were synthesized by the ROP of LA initiated by G4-$(OH)_{32}$. As listed in Table 1, these copolymers are named as Co10–100, in which the number is the ratio of LA monomer to the hydroxyl groups in PEG-G4-$(OH)_{32}$ used in its ROP. For synthesizing Co10, LA (1.0 g, 6.94 mmol) and PEG-G4-$(OH)_{32}$ (500 mg, 0.036 mmol) were weighed in a glove-box and loaded in an oven-dried Schlenk bottle,

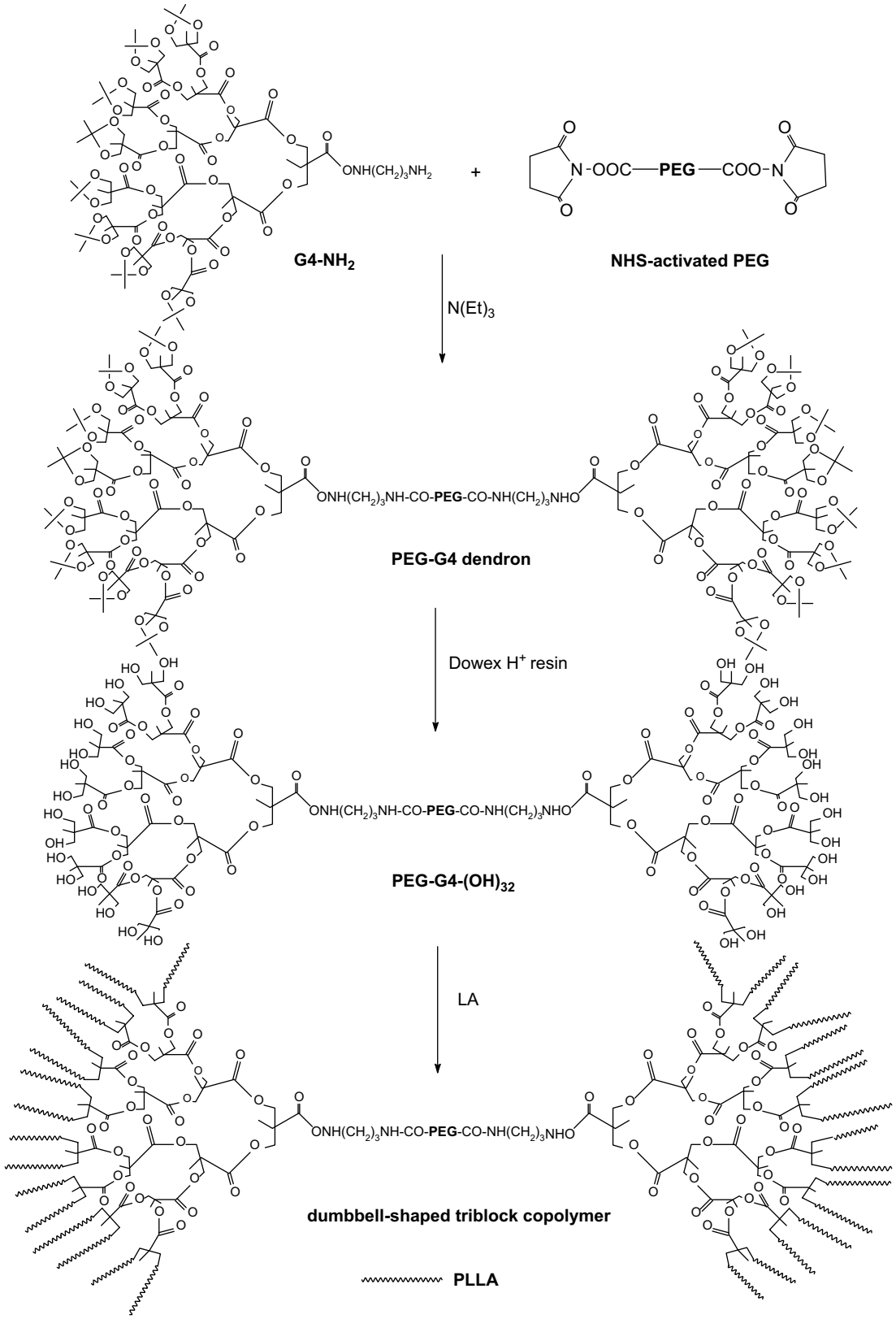

Fig. 1. Synthesis of dumbbell-shaped tri-block copolymers.

5 mg of $Sn(Oct)_2$ (0.5% of LA) was added as a 0.02 g/mL solution in dry CH_2Cl_2. After vacuumized and purged with argon for three times, the bottle was degassed under high vacuum for 2 h to remove the residue of CH_2Cl_2. The bottle was then flame-sealed and immersed in a 130 °C oil bath for 24 h. The obtained white solid was dissolved in CH_2Cl_2 and precipitated in a large amount of chilled methanol. After filtered and dried in vacuum at room temperature, the polymer was recovered with a yield of over 85%.

Table 1
Molecular weights of the copolymers

Sample	$[LA]_0/[OH]_0$	M_n[a]	M_n[b]	M_n[c]	M_w[c]	PDI
Co10	10	56,600	55,400	49,500	52,400	1.06
Co15	15	83,300	79,500	77,100	88,700	1.15
Co50	50	244,600	236,900	204,700	270,200	1.32
Co100	100	475,000	445,700	352,700	515,000	1.46

[a] Calculated from the feed ratio.
[b] Calculated from ^{1}H NMR spectrum.
[c] Obtained from GPC based on the PS calibration.

2.7. Synthesis of LPLLA

LPLLA was synthesized via the ROP of LA in the presence of $Sn(Oct)_2$. LA (14.4 g, 100 mmol) was weighed in a glove-box and introduced to an oven-dried Schlenk bottle, 40 mg of $Sn(Oct)_2$ (0.1 mol% of LA) was added as a 0.02 g/mL solution in dry CH_2Cl_2. After vacuumized and purged with argon three times, the bottle was degassed under a high vacuum for 2 h to remove the residue CH_2Cl_2. The bottle was then flame-sealed and immersed in a 130 °C oil bath for 24 h. The obtained white solid was dissolved in CH_2Cl_2 and precipitated in a large amount of chilled methanol. After dried in vacuum at room temperature, LPLLA with a number average molecular weight (M_n) of 280,000 g/mol and a PDI of 2.0 was recovered with a yield of over 85%.

2.8. Characterizations and measurements

^{1}H NMR spectra were recorded at room temperature on a Bruker DRX-500 using $CDCl_3$ as the solvent. GPC was carried out on a Waters HPLC system equipped with a Model 2690D separation module, a Model 2410 refractive index detector, and Shodex columns (K802.5, K803, and 805). Chloroform was used as the eluent at a flow rate of 1.0 mL/min and calibration was conducted using monodisperse polystyrene (PS) standards. Differential scanning calorimetric (DSC) analysis was carried on a DSC2910 thermal analysis system (TA Instruments Inc., USA) at a heating rate of 10 °C/min under nitrogen atmosphere. Thermogravimetric analysis (TGA) was carried on a TGA2050 thermogravimetric analyzer (TA Instruments Inc., USA) at a heating rate of 20 °C/min from 30 to 500 °C under nitrogen atmosphere. The spherulites formed using the dumbbell-shaped tri-block copolymers were observed using a polarized optical microscope (POM, Nikon ECLIPSE LV100POL). The samples were prepared by casting 1 wt% CH_2Cl_2 solution on clean glass slides and drying for three days at room temperature to remove the residual solvent. The samples were melted at 140, 180, 190, and 200 °C for 3 min separately and then rapidly cooled to their isothermal crystallization temperatures, i.e. the crystalline peak temperature measured in DSC curves, to allow crystallization for 30 min. Finally, the samples were cooled to the room temperature at 10 °C/min and real-time photographs were taken. Surface morphologies of the polymer films were examined by using a scanning electron microscope (SEM, JSM-6360LV, JOEL).

2.9. In vitro cell studies

Polymer films were prepared by dipping clean glass slides in the copolymer solutions in CH_2Cl_2 and evaporating the solvent at room temperature. Contact angle and protein adsorption measurements were carried out using the methods described earlier [52]. In protein adsorption measurements, polymer thin films with a dimension of 1 cm × 1 cm were used and the concentration of adsorbed protein in 750 μL of 1% sodium dodecyl sulfate (SDS) solution was determined using a microplate reader. The viability of rabbit bone marrow stromal cells (BMSCs) after cultured for two days was determined by simultaneous staining with fluorescein diacetate–propidium iodide (FDA–PI). At the blue excitation wavelength of 495 nm, fluorescence microscopic images were taken on the viable and dead cells emitting blue and red fluorescence, respectively. Cell attachment and proliferation were evaluated by seeding human embryonic kidney (HEK) 293T cells (0.9×10^5 cells/mL) on the polymer-coated slides in the Dulbecco's modified Eagle's medium (DMEM, Gibco) supplemented with Newborn Calf Serum (NCS, Gibco) in 12-well tissue culture plates, respectively. Next, 3 mL of medium was added to the wells and mixed with the cells. The cells were then cultured in a humidified incubator equilibrated with 5% CO_2–95% air for four days. The HEK 293T cells attached onto the polymer surfaces were observed using a phase-contrast microscope. The cells were also stained with Hoechst No. 33342 (Sigma) and observed using a fluorescent microscope. Cell proliferation was determined by the MTT assay.

2.10. Statistical analysis

Numerical data are presented as mean ± standard error of the mean. Continuous variables were compared by ANOVA (*t*-test with Bonferroni correction), and categorical variables were compared by χ^2 test. A p value of ≤ 0.05 was considered as significant difference.

3. Results and discussion

3.1. Synthesis and characterizations

Aliphatic polyester dendrons have received much attention in biomedical research because of their biodegradability, highly branching and monodisperse globular shape, well-defined structure, and controlled surface functionality [53]. These unique properties are significantly different from linear polymers and have made them excellent candidates for drug carriers [54]. In this study, the dendritic structure with terminal multi-hydroxyl groups was used to initiate the ROP of LA for the preparation of the dumbbell-shaped tri-block copolymers. The first step was to synthesize amine-terminated fourth-generation dendron shown as G4-NH_2 in Fig. 1. In an earlier work, acetonide-protected polyester dendrons from bis-MPA (generation 1–4) were synthesized according to a strictly divergent method [46]. Attempts to selectively deprotect the benzyl groups can be readily achieved by the catalytic hydrogenolysis because the acetonide protective groups are stable under this condition. The carboxyl-functionalized fourth-generation dendron was then conjugated with 1,3-diaminopropane in the presence of the catalyst CDI to obtain the corresponding amine-terminated molecule. As shown in the first step in Fig. 1, the polyester dendron with a primary amino group at the root was conjugated with NHS-activated PEG. Although the carboxyl terminated polyester dendron can also react with the hydroxyl end groups in ordinary PEG, this direct coupling reaction was less possible because of the steric hindrance effect of the relatively high molecular weight of G4-NH_2 and the low reactivity of the terminal hydroxyl groups in PEG. ^{1}H NMR spectrum of PEG-G4 dendron is shown in Fig. 2. After the coupling reaction, new peaks at ~3.57 ppm can be attributed to the PEG block in the center, indicating the formation of the expected macromolecule.

The average end-capping functionality of PEG with G4 dendron was determined by comparing the integration ratio between the signal b that can be assigned to the dendron unit and the signal of PEG unit at ~3.57 ppm with the theoretical value of 0.0528 for 100% end-capping. In all cases, the ratio larger than 0.95 indicates that all PEG chains have been functionalized with the G4 dendrons

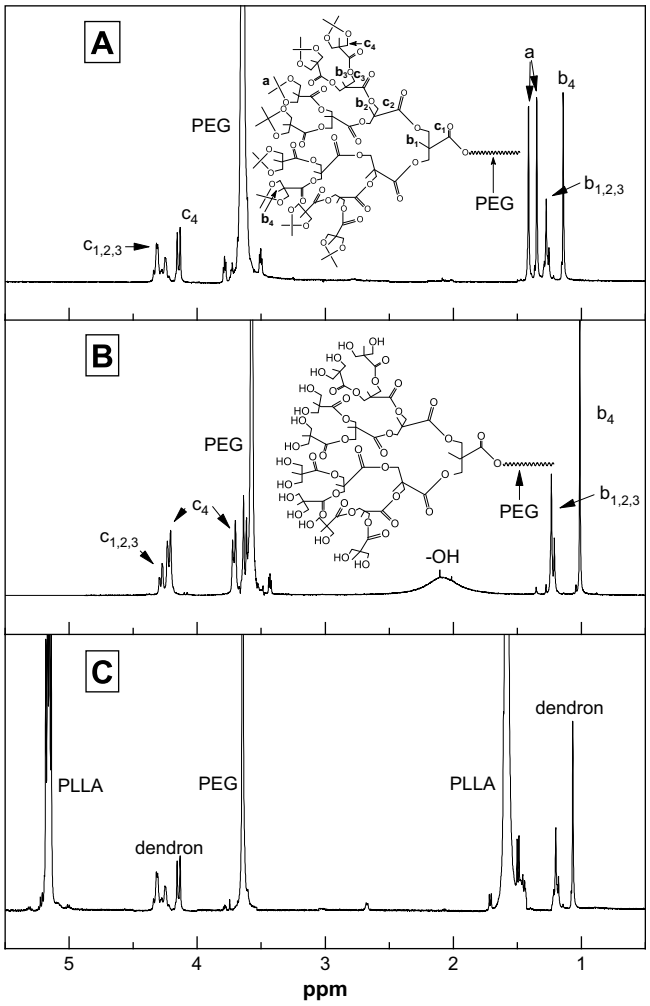

Fig. 2. ^{1}H NMR spectra of (A) PEG-G4 dendron, (B) PEG-G4-$(OH)_{32}$, and (C) Co10.

and it is also confirmed by a symmetrical, monomodal GPC trace with a very small PDI of 1.03 as shown in Fig. 3.

The second step in Fig. 1 is to deprotect the acetonide protective groups at the outer surface of the dendrons. This step was easily realized by the reaction with Dowex H^+ resin at room temperature. This reaction deprotected all acetonide groups without being detrimental to the PEG chains or the dendrons, as supported by the ^{1}H NMR spectrum shown in Fig. 2 and GPC analysis shown in Fig. 3. The peak for the surface methyl groups at 1.34–1.41 ppm completely disappeared while the ratio between other peaks attributed to the dendritic structure and PEG unit remained constant after the deprotection, suggesting no other reactions occurred. Although the loss of surface methyl groups leads to a slight decrease in the polymer molar mass, it cannot be analyzed quantitatively because the interactions between the polymer chains and the solvent could be different after the modification of the terminal groups.

In the third step in Fig. 1, the dumbbell-shaped tri-block copolymers with various PLLA chain lengths were synthesized by the bulk ROP of LA in the presence of terminal dendronized polyhydric PEG macro-initiator and $Sn(Oct)_2$ catalyst at 130 °C. ^{1}H NMR spectrum of the copolymer is illustrated in Fig. 2. The polymerization of LA was carried out under rigorously anhydrous conditions to avoid any initiation by water, which will lead to a mixture of linear and dumbbell-shaped copolymer. The GPC curves of the copolymer shown in Fig. 3 remain monomodal, suggesting no linear PLLA was formed in the copolymerization.

Table 1 lists the GPC results of four dumbbell-shaped tri-block copolymers synthesized using different feed molar ratios of LA monomer and hydroxyl end groups in the macro-initiator PEG-G4-$(OH)_{32}$. The theoretical M_n was calculated from the feed molar ratio $[LA]_0/[OH]_0$ by assuming that all terminal hydroxyl groups initiate the ROP of LA. The molecular weight determined by ^{1}H NMR spectrum was calculated by comparing the signal intensity of methyl protons of PLLA ($\delta = 5.20$ ppm) and that of PEG unit ($\delta = 3.57$ ppm). Because the terminal methyl protons of PLLA ($\delta = \sim 4.30$ ppm) are covered by the dendritic structure, the precise average chain length cannot be obtained. The average length of the PLLA arms was calculated by the molecular weight determined using ^{1}H NMR and the theoretical number of arms, 32. In Fig. 4, the molecular weight of the obtained copolymer increases linearly with the molar ratio $[LA]_0/[OH]_0$, which is consistent with the mechanism for alcohol-initiated ROP.

It is well known that star-shaped polymers have smaller hydrodynamic volumes than linear PS with the same molecular weight [14,55]. Therefore, GPC analysis based on linear monodisperse PS

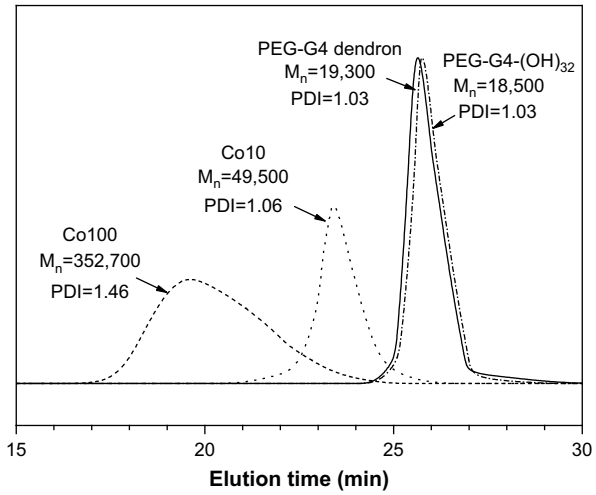

Fig. 3. GPC traces of PEG-G4 dendron, PEG-G4-$(OH)_{32}$, Co10, and Co100.

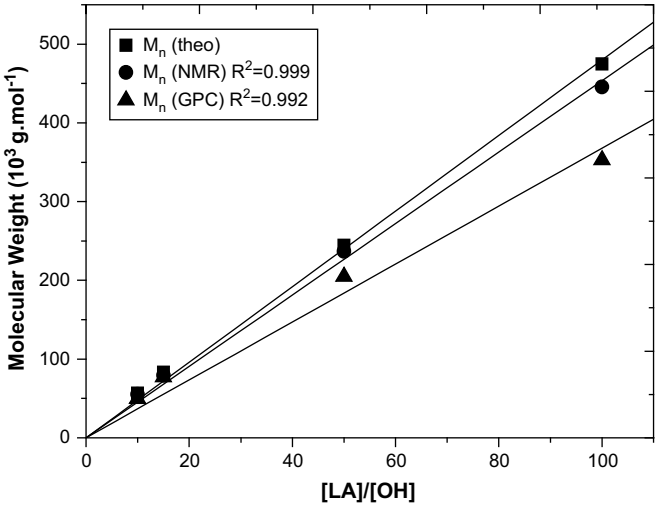

Fig. 4. Molecular weights as functions of the molar ratio of L-lactide (LA) monomer to the hydroxyl groups in PEG-G4-$(OH)_{32}$.

Table 2
Thermal properties of terminally dendronized PEG and dumbbell-shaped tri-block copolymers

Sample	T_g (°C)	T_m (°C)	$\Delta H_m - \Delta H_c$ (J/g)	χ_c (%)	T_d	T_{max}
PEG-G4 dendron	–	56.0	128.4	–	–	–
PEG-G4-$(OH)_{32}$	–	52.9	101.2	–	–	–
Co10	50.8	48.3, 87.3, 122.9	5.0	5.3	252	310
Co15	52.6	158.2	13.9	14.8	260	285
Co50	55.1	167.2	16.3	17.4	265	287
Co100	55.2	174.0	24.1	25.7	271	290
LPLLA	59.4	176.3	32.7	34.8	274	296

standards may not be a satisfactory approach to determine the accurate molecular weights of the dumbbell-shaped tri-block copolymers here. Nevertheless, the molecular weights obtained from ^{1}H NMR spectrum are slightly higher than those GPC data because the center linear PEG block with an M_w of 10,000 g/mol makes the hydrodynamic volume of the dumbbell-shaped polymer close to the linear PS with the same molecular weight.

3.2. Thermal properties and crystalline structure

Table 2 lists the thermal properties of terminal dendronized PEG and dumbbell-shaped tri-block copolymers determined using DSC and/or TGA. Deprotection of the terminal acetonide groups results in a decrease of 3.1 °C in the melting point (T_m) while the thermal stability does not change. Even when the temperature reaches 300 °C, no decomposition can be observed from the DSC curves in Fig. 5. For four dumbbell-shaped tri-block copolymers with different lengths of PLLA arms, their DSC curves, and thermal properties are distinct as shown in Fig. 6 and Table 2. Both crystallization exothermal and melting endothermal peaks appear in the heating run at varied cold crystallization temperature T_{cc} and T_m for Co15, Co50, Co100, and LPLLA. Cold crystallization occurs because the chain motion is allowed for the re-arrangement and packing of crystallizable segments at temperature higher than T_g (but still lower than T_m) in the heating run [52]. For Co10, the melting peak at 48.3 °C for PEG is still discernible in Fig. 6 because of a fairly high composition of PEG center block. In contrast, the other three dumbbell-shaped tri-block copolymers only show melting peaks at the temperatures higher than 150 °C, which are attributed to PLLA arms. T_{cc} decreases from 104.9 °C for Co15 to 91.6 °C for Co50 and 83.6 °C for Co100 as the motions of PLLA arms become less constrained by the center PEG block when they are longer.

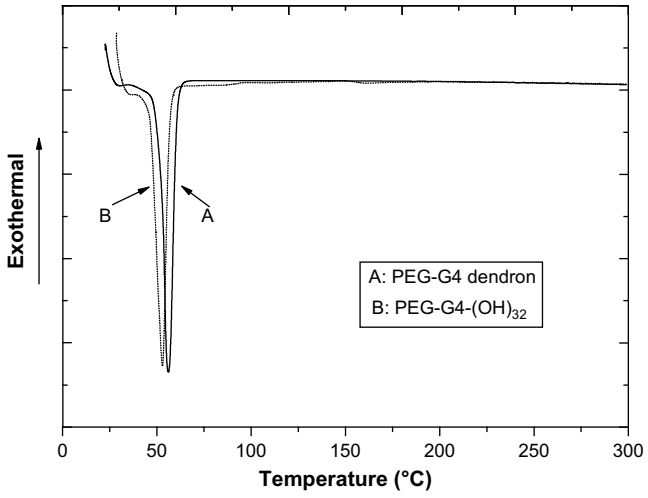

Fig. 5. DSC curves of PEG-G4 dendron and PEG-G4-$(OH)_{32}$.

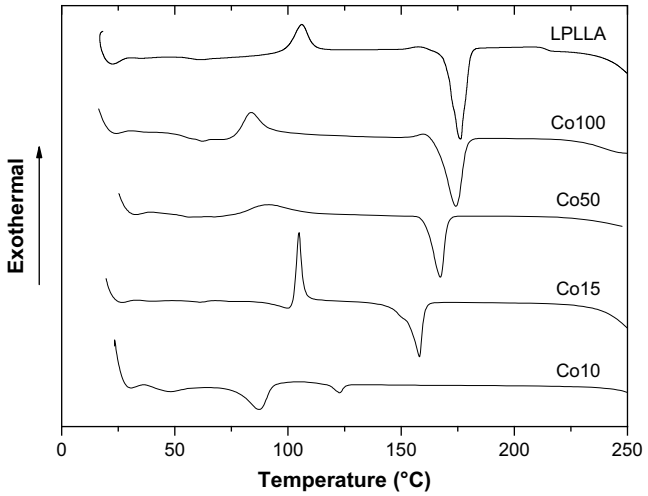

Fig. 6. DSC curves of LPLLA and dumbbell-shaped tri-block copolymers with different lengths of LA arms.

Based on the heats of fusion ΔH_m and ΔH_c obtained from the melting endothermal and crystallization exothermal peaks shown in Fig. 6 and the heat of fusion for 100% crystalline PLLA, $\Delta H_m^0 = 93.6$ J/g, the crystallinity (χ_c) of the copolymer was determined using the equation $\chi_c = (\Delta H_m - \Delta H_c)/\Delta H_m^0$ [14,56]. The glass transition temperature (T_g), T_m, and χ_c of the dumbbell-shaped PLLA are lower than those of LPLLA because of the plasticization of PEG blocks and imperfect crystallinity in the branched structure compared with the linear homopolymer. T_g, T_m, and χ_c increase proportionally with the length of PLLA arms and eventually approach to the values of LPLLA as the PLLA arms are sufficiently long and the PLLA composition is dominant in the copolymers.

POM is often used together with DSC to confirm the crystallization behaviors and thermal properties of novel polymeric systems [57]. The POM images shown in Fig. 7 were taken after the copolymer samples were quenched from isotropic melts to specified crystallization temperatures of 120, 105, 90, 85, and 105 °C for Co10, Co15, Co50, Co100, and LPLLA, respectively. The dumbbell-shaped copolymers exhibit lower rates of nucleation and crystallization compared with LPLLA because of the lower crystallinity in the copolymers. Although both PEG and PLLA blocks are crystallizable, only one type of spherulites from the PLLA block can be observed in the dumbbell-shaped copolymers as shown in Fig. 7. In an earlier report, PLLA–PEG di-block copolymers were revealed to form spherulites with banded textures [58]. For dumbbell-shaped tri-block copolymers of PEG and PLLA crystallized at the studied temperatures, only spherulites with clear Maltese cross can be observed except Co10 that has a rather small crystallintiy of 5.3%. The POM images are consistent with the DSC data as there is only one endothermic melting peak in the heating run and one exothermal crystallization peak in the cooling run, indicating that only one block can be crystallized. The fact that PEG and PLLA crystals cannot co-exist in the copolymers can be interpreted as that the PLLA blocks can form folded lamellar single crystals while PEG blocks are still amorphous at the crystallization temperatures not lower than 85 °C [58]. In addition, the PEG blocks are double covalently connected to the PLLA dendrons, their motion and rearrangement are greatly prohibited and the macroscopic phase separation from the PLLA lamellae is not preferred energetically.

Thermal stability of the copolymers was analyzed by TGA. As shown in Fig. 8 and Table 2, the onset decomposition temperature

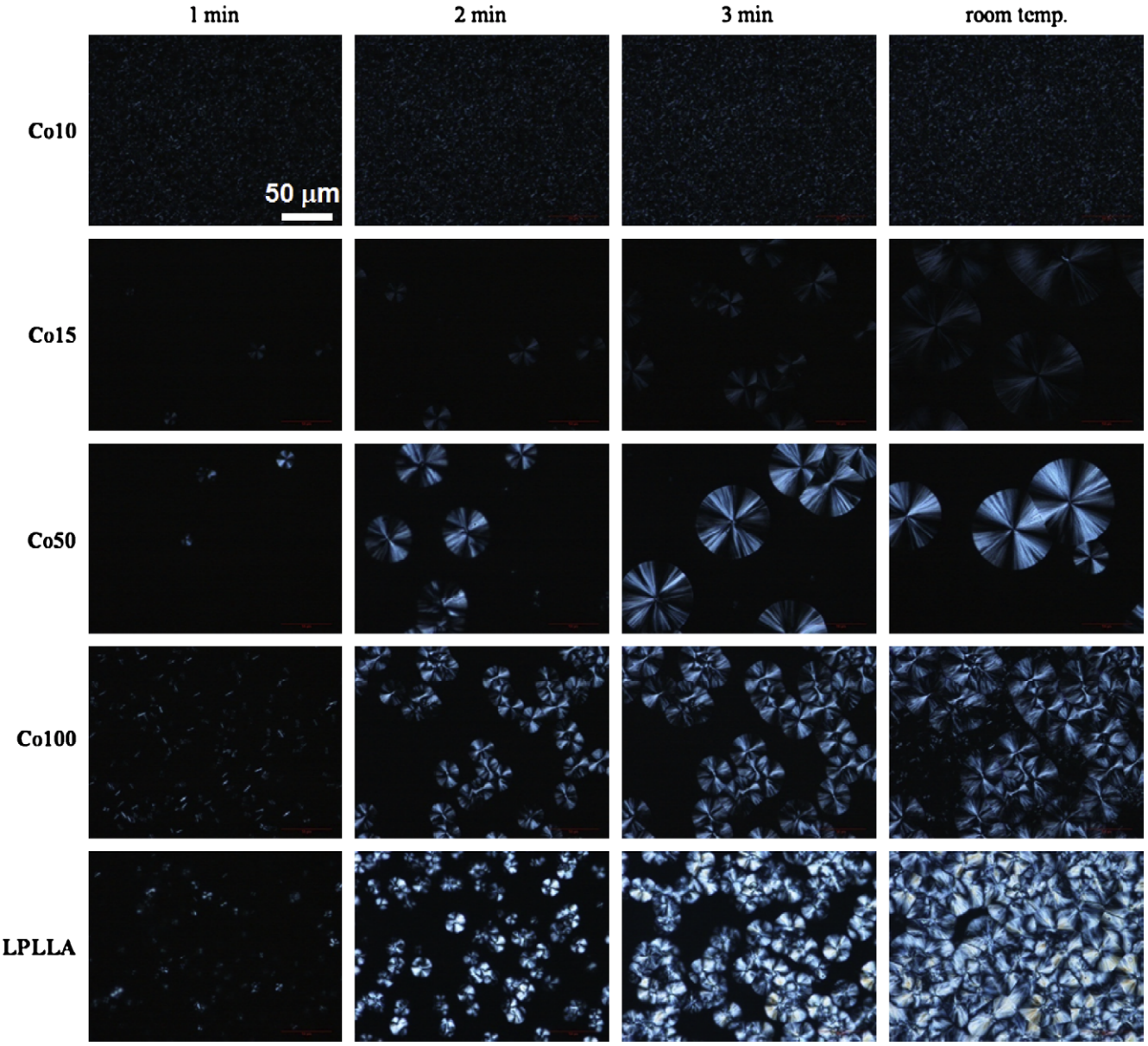

Fig. 7. POM images of LPLLA and dumbbell-shaped copolymers crystallized at their crystallization peak temperatures determined by DSC curves for 1, 2, 3 min and then cooled at room temperature. The scale bar in Co10 at 1 min stands for 50 μm and it is applicable for all.

(T_d) of the dumbbell-shaped copolymer increases with the length of PLLA arms up to the value of 274 °C for LPLLA. T_{max} determined from the maximum degradation rate peak in derivative thermogravimetry (DTG) thermograms (not shown) also increases with the molecular weight except Co10, which has lowest T_d but the highest T_{max} among these four copolymers and LPLLA. It can be explained by a two-step decomposition process. The first step can be attributed to the decomposition of PLLA segments while the second one is attributed to PEG segments. In Co10, the high density of thermal unstable terminal hydroxyl groups of PLLA chain and low molecular weight led to a faster decomposition to form cyclic monomer with a low T_d [59]. As reported earlier, PEG with a nominal molecular weight of 10,000 g/mol has a T_d at 405 °C [60], which is much higher than 274 °C for LPLLA. When the decomposition continues, the composition of the thermally more stable PEG center block increases and consequently T_{max} is higher than those of the other copolymers and LPLLA.

3.3. Surface morphology and chemistry

Fig. 9 shows the surface morphology of the dumbbell-shaped copolymer films before and after steam sterilization in an autoclave. The films were fabricated by casting 0.02 g/mL polymer/CH_2Cl_2 solution onto the glass slides and evaporating the solvent directly at room temperature. As shown in Fig. 9A1, the surface of Co10 was smooth without any pores and the film was transparent. With increasing the length of PLLA arms, the copolymer surface became rougher and semi-porous structures with larger pore size were formed progressively. It is well known that the "breath figure" method can generate ordered structure porous polymer films by evaporating volatile organic solvent under humid condition [61–63]. PLLA/PEG blend films with porous upper surface were reported previously after solution casting and solvent evaporation [64,65]. Similar to these cases revealed earlier [61–65], the formation of porous structure using the dumbbell-shaped amphiphilic

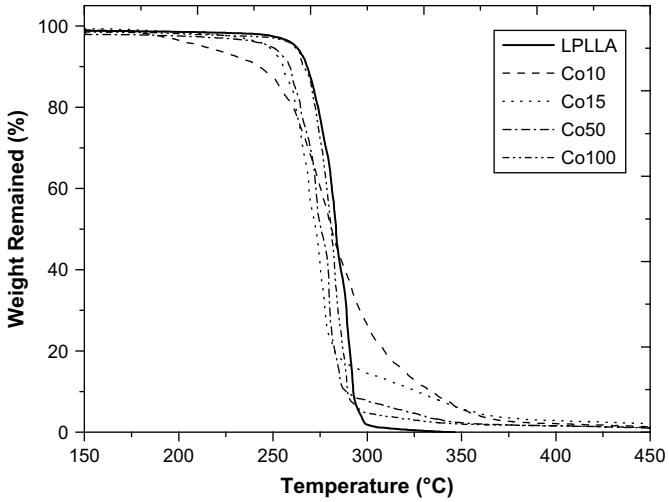

Fig. 8. TGA thermograms of LPLLA and dumbbell-shaped tri-block copolymers.

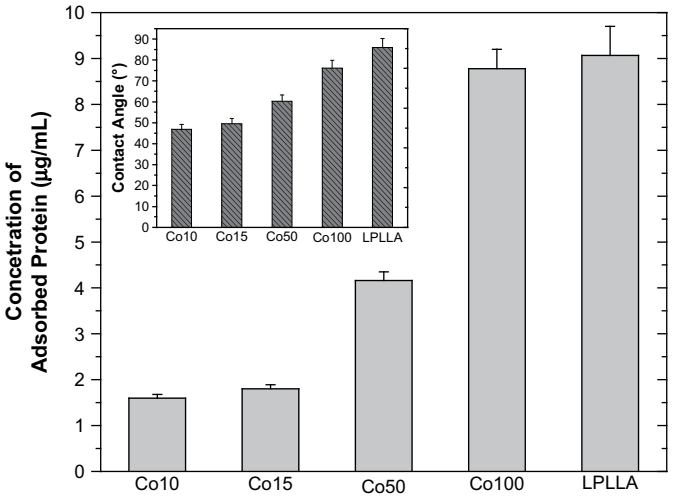

Fig. 10. Protein adsorption and contact angles (inset) on the surface of LPLLA and dumbbell-shaped copolymers.

copolymers are related to the rapid evaporation of solvent, condensation of water droplets at the surface, and microphase separation of the two blocks with hydrophobic and hydrophilic characteristics. Although humid condition was not given specifically, the air surrounding the polymer solution contained moisture during the solvent evaporation. Because water droplets only stabilized on the surface of the polymer solution, pores were formed on the top layers of the films while the bottom of the films was still solid and smooth.

Since the copolymer samples for cell studies were used after steam sterilization in an autoclave, the surface morphology of the copolymer films after sterilization at elevated temperature of ~120 °C and then crystallization was also examined by using SEM. As shown in Fig. 9B, the porous structure of the film surface became more evident especially for Co50, in which the pores were significantly larger (~5 mm) compared to the untreated film in Fig. 9A3. Nevertheless, the trend still remains that the surface became rougher with larger pore area when the length of PLLA arms increases. Highly ordered honeycomb surface can be achieved when the $[LA]_0/[OH]_0$ ratio is greater than 100. The effects of PLLA arm length, copolymer concentration, and solvent quality on the surface pattern parameters are under investigation and the results will be reported soon.

Like surface morphology, surface chemistry is another key factor in influencing cell responses [66]. Two characteristic parameters of surface chemistry, hydrophobicity and the capability of adsorbing proteins from cell culture medium, have been determined and demonstrated in Fig. 10. The inset in Fig. 10 indicates that the water contact angle increases from 46.8° for Co10 to 76.1° for Co100, which is still lower than the value of 86° for LPLLA. It is believed that a more hydrophobic polymer surface is more favorable for protein adsorption and a rougher surface having more surface area can adsorb more protein from cell culture medium [66]. Meanwhile, a water contact angle around 50° is believed to be more favorable for cell attachment than too hydrophilic or too hydrophobic surfaces [66]. With increasing the PLLA arm length in the dumbbell-shaped copolymers, the above-mentioned two parameters change in a favorable direction to enhance protein adsorption, as observed in Fig. 10. Evidently, introducing the hydrophilic PEG

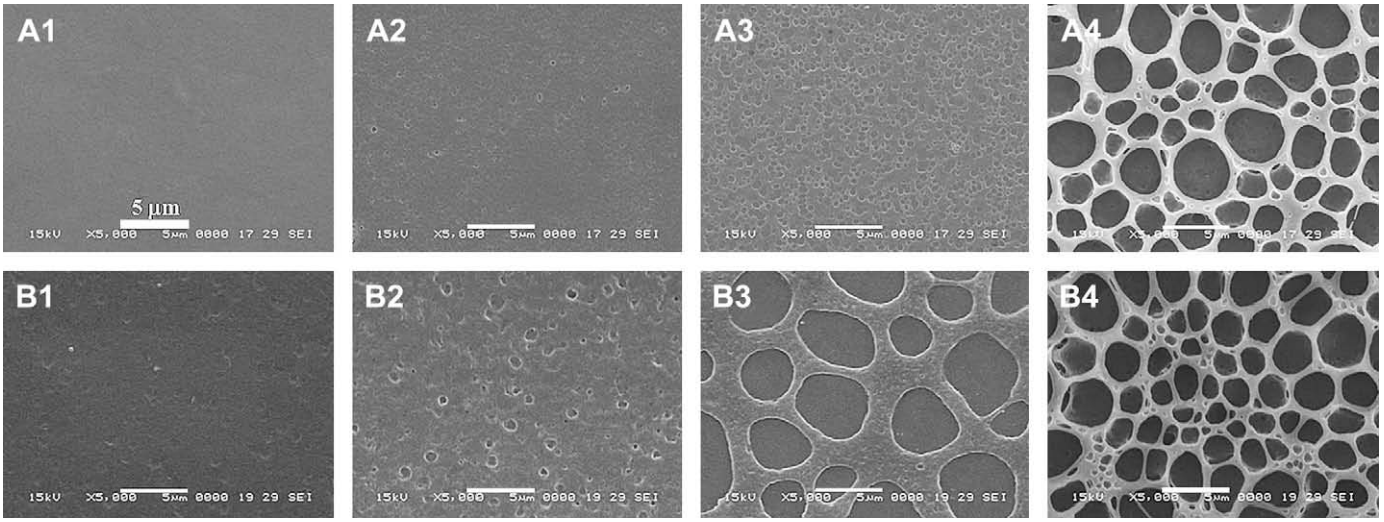

Fig. 9. Scanning electron micrographs of the surfaces of dumbbell-shaped copolymer films (A) before and (B) after sterilization in an autoclave. 1: Co10, 2: Co15, 3: Co50, 4: Co100. The scale bar in A1 stands for 5 μm and is applicable for all.

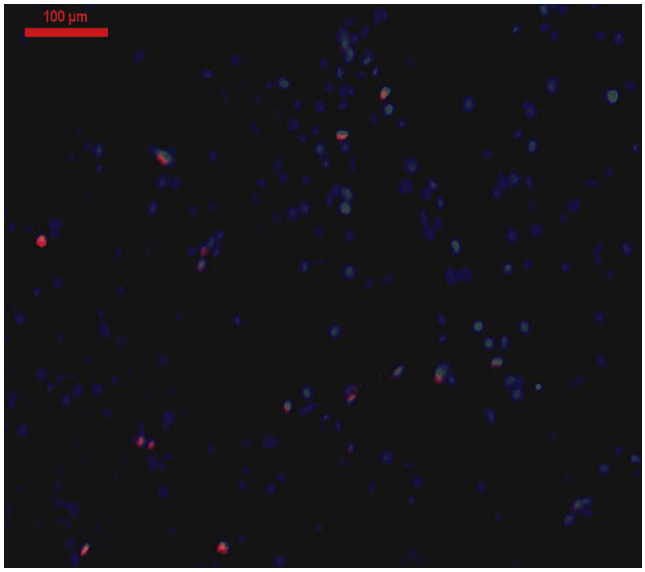

Fig. 11. A typical microscopic image of rabbit bone marrow stromal cells seeded on the film surface of dumbbell-shaped Co10 48 h post-seeding, where viable cells were stained in blue fluorescence while dead cells in red. The scale bar stands for 100 μm.

center block to two PLLA dendrons is an efficient method to regulate polymer hydrophilicity and protein adsorption as well as the surface roughness discussed earlier.

3.4. In vitro cell responses

In order to explore diverse tissue-engineering applications of these novel dumbbell-shaped tri-block copolymers, preliminary studies have been performed to evaluate their *in vitro* cell compatibility using rabbit BMSCs, and cell attachment and proliferation on the copolymer surfaces using HEK 293T cells. In Fig. 11, viable rabbit BMSCs were stained in blue while dead cells were stained in red (For interpretation of the references to color in the text and in the figure legend, the reader is referred to the web version of this article.). As exemplified by using Co10, rabbit BMSCs adhered to and proliferated on the polymer surfaces 48 h post-seeding with high viabilities above 98% without significant difference among different polymers ($p > 0.05$). It indicates all these five polymer samples in Table 2 have excellent compatibility with rabbit BMSCs.

There are three major factors in influencing cell/biomaterial interactions: surface chemistry, surface topology, and mechanical properties [66]. As demonstrated in Figs. 9 and 10, surface roughness, hydrophobicity, and the capability of adsorbing protein all vary with the chemical composition of the dumbbell-shaped

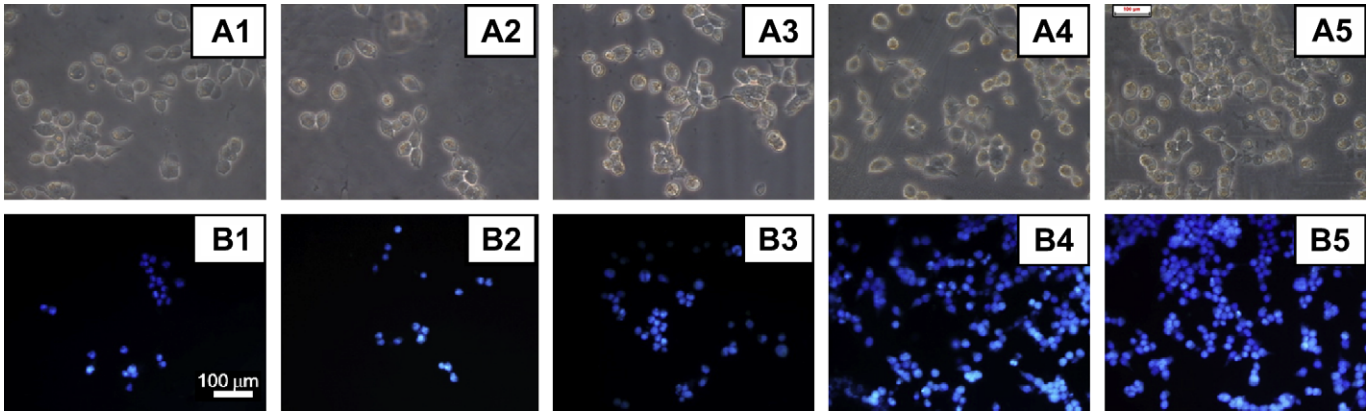

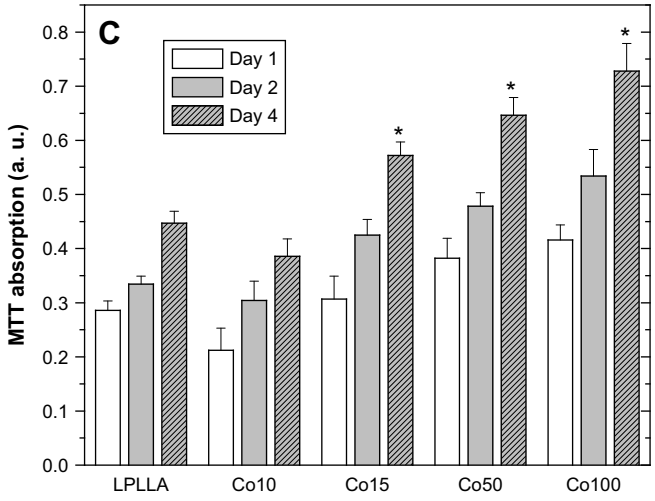

Fig. 12. HEK 293T cell attachment and proliferation on LPLLA (A1, B1) and four dumbbell-shaped copolymers (A, B2–5: Co10, Co15, Co50, Co100). (A) Phase-contrast micrographs of attached HEK 293T cells four days post-seeding. (B) Nuclei of attached HEK 293T cells stained by using Hoechst No. 33342 and visualized by a fluorescence microscope four days post-seeding. (C) MTT absorption for 1, 2, 4 days. The scale bar in B1 stands for 100 μm and it is applicable for all micrographs in (A) and (B). In panel (C), no significant difference ($p > 0.05$) is between LPLLA and Co10. $^{*}p < 0.05$ between LPLLA or Co10 and Co15, Co50, Co100 at day 4.

copolymers in a correlative way. Furthermore, the general trends in these chemical and topological factors are positive in supporting cell attachment and proliferation. The role of surface stiffness has been revealed in regulating cell responses using numerous polymeric systems and a higher surface stiffness can enhance cell proliferation [52,66,67]. The mechanical properties such as tensile modulus and surface stiffness were reported to increase with the PLLA composition in the copolymers or blends consisting of PLLA and PEG [68]. For the dumbbell-shaped copolymers in this study, thin films made from Co10 and Co15 are very weak and cannot even stand a very small tension. As the molecular weight of PLLA arms increases, the mechanical properties increase significantly. The tensile modulus, stress at break, and strain at break were measured to be 1.87 ± 0.14 GPa, 46 ± 13 MPa, and $36.6 \pm 8.2\%$ for Co50 and 2.46 ± 0.18 GPa, 67 ± 17 MPa, and $16.7 \pm 3.7\%$ for Co100, respectively. Therefore, enhanced cell proliferation can be expected to occur in the dumbbell-shaped tri-block copolymers with longer PLLA arms or higher PLLA compositions, considering all the determining factors will be favorable for it.

Fig. 12 shows both cell morphology and MTT absorption for HEK 293T cells. Fig. 12A and B demonstrates that the number of attached HEK 293T cells on the tri-block copolymer surface four days post-seeding increases evidently with the length of PLLA arm, which is consistent with the MTT absorption data in Fig. 12C. Furthermore, the dumbbell-shaped tri-block copolymers except Co10 show significantly enhanced HEK 293T cell proliferation than LPLLA, which is widely used as a biomaterial for tissue-engineering and drug-delivery applications. The adhesion and proliferation of cells on these materials also indicate no cytotoxicity of the copolymers. The cell viability was still maintained as high as 100% although there were fewer cells adhered on the surface of Co10. The cell responses to the copolymers as shown in Fig. 12 are in agreement with each other and can be very well interpreted by the earlier discussion on the material properties that influence cell behavior. Similar trend can be found in the proliferation of human vein endothelial cells (HUVEC) when seeded on the copolymers and LPLLA.

In some applications, surfaces are required to resist cell adhesion and proliferation. This goal can be reached by introducing hydrophilic PEG center block to the hydrophobic, more rigid PLLA blocks to obtain copolymers with fairly lower protein adsorption and less rough surface. Beyond the scope of this report, the degradation of these novel comb-dendritic tri-block copolymers and their applications in drug delivery are being investigated and will be reported subsequently. Furthermore, comprehensive studies on the self-assembled structures using this series of dumbbell-shaped tri-block copolymers are being conducted in our group. As mentioned earlier, honeycomb surface patterns could be formed using the copolymers with PLLA arm length longer than those presented in this report. Such honeycomb surface pattern can be regulated by a few factors such as the polymer concentration and solvent quality. In dilute solutions, we recently found that these amphiphilic dumbbell-shaped tri-block copolymers can form self-assembled micro-fibrils. The effects of these controllable topological features on 2D and 3D cell responses will enable us to better understand both polymer science and biomaterials [69,70].

4. Conclusions

A series of well-defined dumbbell-shaped tri-block copolymers of comb-like polylactide (PLLA) and linear polyethylene glycol (PEG) with narrow molecular weight distributions and varied PLLA arm lengths have been synthesized through the bulk ring-opening polymerization of L-lactide (LA) in the presence of terminal dendronized polyhydric PEG macro-initiator and $Sn(Oct)_2$ catalyst at 130 °C. The length of PLLA arms can be readily controlled by the feed molar ratio of LA to the hydroxyl groups in the PEG macro-initiator. The glass transition temperature (T_g), melting point (T_m), crystallinity (χ_c), and onset decomposition temperature (T_d) of the copolymer are lower than those of linear polylactide (LPLLA). When the PLLA composition in the copolymer is sufficiently high, porous structures can be formed on the top layers of the copolymer films after solution casting and solvent evaporation. Surface hydrophobicity and the capability of adsorbing protein from the cell culture medium increase with the length of PLLA arms. The copolymers have no cytotoxicity to rabbit bone marrow stromal cells. Benefited from the collective favorable factors of rougher surface, better capability of adsorbing protein, and higher surface stiffness, significantly enhanced cell proliferation on the copolymers with longer PLLA arm lengths was found using HEK 293T cells. Efficient regulation of material properties and cell responses thus can be achieved using this series of dumbbell-shaped tri-block copolymers, suggesting their great potentials for various tissue-engineering applications.

Acknowledgments

This work was supported by the 863 Project (2007AA02Z450) from the Ministry of Science and Technology of China. We thank Shanghai Aosi Biological Technology Service Co., Ltd. for the gift of cells and technical assistance for cell culture.

References

[1] Yang Y, Bajaj N, Xu PS, Ohn K, Tsifansky MD, Yeo Y. Biomaterials 2009; 30(10):1947–53.
[2] Nasongkla N, Shuai X, Ai H, Brent DW, John P, David AB, et al. Angew Chem Int Ed 2004;43:6323–7.
[3] Ouchi T, Toyohara M, Arimura H, Ohya Y. Biomacromolecules 2002;3:885–8.
[4] Deng C, Tian HY, Zhang PB, Sun J, Chen XS, Jing XB. Biomacromolecules 2006;7:590–6.
[5] Li SM, Garreau H, Pauvert B, McGrath J, Toniolo A, Vert M. Biomacromolecules 2002;3:525–30.
[6] Kwon GS, Kataoka K. Adv Drug Deliv Rev 1995;16:295–309.
[7] Li SM, Liu LJ, Garreau H, Vert M. Biomacromolecules 2003;4:372–7.
[8] Tabata Y. Pharm Sci Technol Today 2000;3:80–9.
[9] Sheridan MH, Shea LD, Peters MC, Mooney DJ. J Control Release 2000;64: 91–102.
[10] Baldwin SP, Saltzman WM. Adv Drug Deliv Rev 1998;33:71–86.
[11] Whang KM, Goldstick TK, Healy KE. Biomaterials 2000;21:2545–51.
[12] Breitenbath A, Kissel T. Polymer 1998;39:3261–71.
[13] Luo YF, Wang YL, Niu XF, Shang JF. Eur Polym J 2008;44:1390–402.
[14] Zhao YL, Cai Q, Jiang J, Shuai XT, Bei JZ, Chen CF, et al. Polymer 2002;43: 5819–25.
[15] Li YX, Volland C, Kissel T. Polymer 1998;39:3087–97.
[16] Breitenbach A, Pistel KF, Kissel T. Polymer 2000;41:4781–92.
[17] Cai Q, Zhao YL, Bei JZ, Xi F, Wang SG. Biomacromolecules 2003;4:828–34.
[18] Chen HT, Neerman MF, Parrish AR, Simanek EE. J Am Chem Soc 2004; 126:10044–8.
[19] Okuda T, Kawakami S, Akimoto N, Niidome T, Yamashita F, Hashida M. J Control Release 2006;116:330–6.
[20] Okuda T, Kawakami S, Maeie T, Niidome T, Yamashita F, Hashida M. J Control Release 2006;114:69–77.
[21] Gillies ER, Dy E, Fréchet JMJ, Szoka FC. Mol Pharm 2005;2:129–38.
[22] Gillies ER, Fréchet JMJ. J Am Chem Soc 2002;124:14137–46.
[23] Guillaudeu SJ, Fox ME, Haidar YM, Dy EE, Szoka FC, Fréchet JMJ. Bioconjug Chem 2008;19:461–9.
[24] Cai Q, Wan YQ, Bei JZ, Wang SG. Biomaterials 2003;24:3555–62.
[25] Finne A, Albertsson AC. Biomacromolecules 2002;3:684–90.
[26] Kricheldorf HR, Hachmann TH, Schwarz G. Biomacromolecules 2004;5:492–6.
[27] Ydens I, Degée P, Dubois P, Libiszowski J, Duda A, Penczek S. Macromol Chem Phys 2003;204:171–9.
[28] Teramoto Y, Nishio Y. Polymer 2003;44:2701–9.
[29] Nouvel C, Dubois P, Dellacherie E, Six JL. J Polym Sci Part A: Polym Chem 2004;42:2577–88.
[30] Du YJ, Lemstra PJ, Nijenhuis AJ, Van Aert HAM, Bastiaansen C. Macromolecules 1995;28:2124–32.
[31] Yang JL, Zhao T, Zhou YC, Liu LJ, Li G, Zhou EL, et al. Macromolecules 2007; 40:2791–7.
[32] Yasugi KJ, Nakamura T, Nagasaki Y, Kato M, Kataoka K. Macromolecules 1999; 32:8024–32.

[33] Han DK, Hubbell JA. Macromolecules 1997;30:6077–83.
[34] Fujiwara T, Kimura Y. Macromol Biosci 2002;2:11–23.
[35] Schindler A, Hibionada YM, Pitt CG. J Polym Sci Part A: Polym Chem 1982; 20:319–26.
[36] Zhang XC, MacDonald DA, Mattheus FA, McAuley GKB. J Polym Sci Part A: Polym Chem 1994;32:2965–70.
[37] Nijenhuis AJ, Grijpma DW, Pennings AJ. Macromolecules 1992;25:6419–24.
[38] Ryner M, Stridsberg K, Albertsson AC, Von Schenck H, Svensson M. Macromolecules 2001;34:3877–81.
[39] Kowalski A, Duda A, Penczek S. Macromolecules 2000;33:689–95.
[40] Gottschalk G, Frey H. Macromolecules 2006;39:1719–23.
[41] Numata K, Srivastava RK, Finne WA, Albertsson AC, Doi Y, Abe H. Biomacromolecules 2007;8:3115–25.
[42] Yuan WZ, Yuan J, Zheng S, Hong X. Polymer 2007;48:2585–94.
[43] Korhonen H, Helminen A, Seppälä JV. Polymer 2001;42:7541–9.
[44] Frauenrath H. Prog Polym Sci 2005;30:325–84.
[45] Bayer U, Stadler R. Macromol Chem Phys 1994;195:2709–22.
[46] Malkoch M, Malmstrom E, Hult A. Macromolecules 2002;35:8307–14.
[47] Walach W, Trzebicka B, Justynska J, Dworak A. Polymer 2004;45:1755–62.
[48] Washio I, Shibasaki Y, Ueda M. Macromolecules 2005;38:2237–46.
[49] Tian L, Hammond PT. Chem Mater 2006;18:3976–84.
[50] Peng S-M, Chen Y, Hua C, Dong CM. Macromolecules 2009;42:104–13.
[51] Moore JS, Stupp SI. Macromolecules 1990;23:65–70.
[52] Wang SF, Kempen DH, Simha NK, Lewis JL, Windebank AJ, Yaszemski MJ, et al. Biomacromolecules 2008;9:1229–41.
[53] Fréchet JMJ. Science 1994;263:1710–5.
[54] Cordova A, Janda KD. J Am Chem Soc 2001;123:8248–59.
[55] Aoi K, Hatanaka T, Tsutsumiuchi K, Okada M, Imae T. Macromol Rapid Commun 1999;20:378–82.
[56] Cohn D, Younes H, Marom G. Polymer 1987;28:2018–22.
[57] Wang SF, Lu LC, Gruetzmacher JA, Currier BL, Yaszemski MJ. Macromolecules 2005;38:7358–70.
[58] Sun JR, Hong ZK, Yang LX, Tang ZH, Chen XS, Jing XB. Polymer 2004;45: 5969–77.
[59] Jamshidi K, Hyon SH, Ikada Y. Polymer 1988;29:2229–34.
[60] Wang SF, Lu LC, Gruetzmacher JA, Currier BL, Yaszemski MJ. Biomaterials 2006;27:832–41.
[61] François B, Pitois O, François J. Adv Mater 1995;7:1041–4.
[62] Srinivasarao M, Collings D, Philips A, Patel S. Science 2001;292:79–83.
[63] Yabu H, Shimomura M. Chem Mater 2005;17:5231–4.
[64] Nakane K, Hata Y, Morita K, Ogihara T, Ogata N. J Appl Polym Sci 2004;94: 965–70.
[65] Swaminathan V, Tchao R, Jonnalagadda S. J Biomater Sci Polym Ed 2007; 18:1321–33.
[66] Harbers GM, Grainger DW. Cell-material interactions: fundamental design issues for tissue engineering and clinical considerations. In: Guelcher SA, Hollinger JO, editors. Introduction to biomaterials. Boca Raton: CRC Press; 2005. p. 15–45.
[67] Discher DE, Janmey P, Wang YL. Science 2005;310:1139–43.
[68] Chen W, Yang J, Wang S, Bei J. Acta Polym Sin 2002;5:695–702.
[69] Arai K, Tanaka M, Yamamoto S, Shimomura M. Colloid Surf A 2008;313–314:530–5.
[70] Tanaka M, Nishikawa K, Okubo H, Kamachi H, Kawai T, Matsushita M, et al. Colloid Surf A 2006;284-5:464–9.